# Multimodal Diagnosis using Deep Fuzzy Cognitive Map with Extreme Learning Machine Integrated into a Medical Decision Support System for Coronary Artery Disease and Non-Small Cell Lung Cancer Detection

Elpiniki Papageorgiou
Dept of Energy Systems
University of Thessaly
Larisa, Larisa, Greece
elpinikipapageorgiou@uth.gr

Anna Feleki
Dept of Energy Systems
University of Thessaly
Larisa, Larisa, Greece
annafele1@uth.gr

Nikolaos Papandrianos*
Dept of Energy Systems
University of Thessaly
Larisa, Larisa, Greece
npapandrianos@uth.gr

Ioannis Apostolopoulos
Dept of Energy Systems
University of Thessaly
Larisa, Larisa, Greece
ece7216@upnet.gr

Konstantinos Papageorgiou
Dept of Energy Systems
University of Thessaly
Larisa, Larisa, Greece
konpapageorgiou@uth.gr

Nikolaos Papathanasiou
School of Medicine
University of Patras
Patras, Greece
nikopapath@upatras.gr

Dimitrios Apostolopoulos
School of Medicine
University of Patras
Patras, Patra, Greece
dimap@upatras.gr

## Abstract

Early detection of Coronary Artery Disease (CAD) and Non-Small Cell Lung Cancer (NSCLC) is crucial for improving patient outcomes. In this study, RGB-CNN (Convolutional Neural Network) was implemented, and trained from scratch using Polar Maps for CAD diagnosis and Computed Tomography (CT) images for NSCLC diagnosis. The CNN predictions were then integrated with clinical data into a Fuzzy Cognitive Map (FCM) classifier for each type of diagnosis. Nuclear medicine experts provided linguistic values in the form of fuzzy sets to define the relationships between input and output concepts, which were later converted into interval values. Extreme Learning Machine (ELM) and Genetic Algorithm (GA) were applied to the FCM learning process to refine the interconnections based on expert knowledge. To ensure the robustness of the results, 10-fold cross-validation was employed. The DeepFCM-ELM model demonstrated superior performance, achieving 80.4%±4.97% accuracy for CAD diagnosis, and 91.9%±3.07% for NSCLC diagnosis using CT images. Heatmaps were generated to interpret CNN predictions by highlighting pathological regions. These heatmaps were then used in GPT, along with DeepFCM weights, CNN, and DeepFCM prediction and input clinical values, employing Natural Language Generation to translate DeepFCM results into human-readable language, enhancing the model's overall explainability. All these techniques have been integrated into a Medical Decision Support System (MDSS) designed to effectively manage both medical classification challenges.

## CCS Concepts

• **Fuzzy Cognitive Maps**; • **Extreme Learning Machine**; • **Deep Learning**;

## Keywords

Medical classification, Convolutional neural networks, Coronary artery disease, Non-small cell lung cancer

**ACM Reference Format:**
Elpiniki Papageorgiou, Anna Feleki, Nikolaos Papandrianos, Ioannis Apostolopoulos, Konstantinos Papageorgiou, Nikolaos Papathanasiou, and Dimitrios Apostolopoulos. 2024. Multimodal Diagnosis using Deep Fuzzy Cognitive Map with Extreme Learning Machine Integrated into a Medical Decision Support System for Coronary Artery Disease and Non-Small Cell Lung Cancer Detection. In *28th Pan-Hellenic Conference on Progress in Computing and Informatics (PCI 2024), December 13–15, 2024, Egaleo, Greece.* ACM, New York, NY, USA, 7 pages. https://doi.org/10.1145/3716554.3716615

*Corresponding Author.



*PCI 2024, Egaleo, Greece*

ACM ISBN 979-8-4007-1317-0/2024/12
https://doi.org/10.1145/3716554.3716615

## 1 Introduction

Coronary Artery Disease (CAD) is the most common type of heart disease [13]. CAD refers to the blockage of coronary arteries, which supply blood to the myocardium, due to the plaque constructed on the inner walls of the arteries. This leads to stenosis of arteries, which limits the circulation of the blood flow to the myocardium, which can cause ischemic episodes [14]. Lung cancer is the leading

cause of cancer-related deaths, where approximately 85% of which are Non-Small Cell Lung Cancer (NSCLC). Since NSCLC does not present early symptoms the majority of NSCLC lesions are at advanced stage, by the time they are detected. For both case studies, early detection and timely intervention are fundamental, for decreasing mortality and selecting the appropriate treatment for each patient. The diagnostic methods that are currently in use are often invasive, expensive, time-consuming, and can pose risks for patients. Artificial intelligence (AI) has implemented techniques that offer high accuracy and efficiency. Deep learning, machine learning, and fuzzy cognitive map models can analyze large datasets, including medical instances and clinical information, to detect early signs of diseases [8].

The following literature review includes related studies regarding the early diagnosis of CAD and NSCLC. Regarding CAD diagnosis, in the study [2] the authors proposed different ensemble-learning frameworks to detect different types of heart disease, with CNN, Long-Short Term Memory, (LSTM), bidirectional LSTM (BiLSTM), Gated Recurrent Unit (GRU), bidirectional GRU (BiGRU). The dataset consisted of 800 records, describing the biological indicators of the patients including age, sex, heart rate, etc. Preprocessing techniques were applied with the min-max normalization techniques and three different subsets were generated from different feature selection methods. Furthermore, to handle the imbalance of the dataset averaging, random under-balancing methods were applied to generate instances to balance the dataset equally. Based on the results, an ensemble classifier with BiLSTM or BiGRU model with a CNN model attained the best performance metrics with accuracy and F1-score between 91% and 96% for the different types of heart disease. In the study [1] the authors aimed to detect CAD and evaluate patient risk, by applying different feature selection methods and machine learning algorithms, to find the optimal combination. 395 patients were included in this study, with rest/stress myocardial perfusion SPECT images demonstrating each instance. Segmentation was applied to manually extract the left ventricle myocardium, where 118 radiomics features were extracted. Nuclear physicians classified the instances into normal and CAD and low, intermediate, and high-risk groups. The dataset included 78 normal and 317 CAD patients, including 135 low, 12 intermediate, and 55 high-risk patients, where normalization was applied with the Z-score, and to handle the imbalance Synthetic Minority Over-sampling Technique (SMOTE) was applied to selected features. Diabetes demonstrated the highest correlation for cardiovascular events. For both tasks, it seemed that the feature sets attained from the Stress images demonstrated better the CAD pathology. For the first task, stress-mRMR-KNN yielded the best results with values of AUC, accuracy, sensitivity, and specificity of 0.61, 0.63, 0.64, and 0.6 respectively, and for the second task, stress-Boruta-GB achieved 0.79, 0.76, 0.75 and 0.76 accordingly. Concerning the NSCLC diagnoses, advanced techniques have been implemented with CT scans explored aiming at improving accuracy and efficiency. In [12] the aim was to classify NSCLC into adenocarcinoma and squamous cell carcinoma. In this work, dense neural networks (VGG-16 and ResNet-50) and sparse neural network (Inception v3) were applied and compared for the diagnosis of NSCLC. A total of 120 patients were utilized for the classification of NSCLC, with CT images, where 60 patients were initially classified by nuclear experts with adenocarcinoma and 60 patients with squamous cell carcinoma. The CT images have a pixel size of 512x512. The trained models were validated with the LC25000 dataset, where the Inception-V3 network outperformed them with sensitivity, specificity, and accuracy values of 96.66%, 99.12%, and 98.29% respectively. It seems that the current literature studies do not offer transparency behind the decision-making process of the proposed models.

The novelty of this research study is to provide an explainable method for CAD and NSCLC diagnosis and include Extreme Learning Machine in the training process of DeepFCM. DeepFCM has been developed and published in previous studies [4]. As part of the EMERALD project, the MDSS system has been developed [15], and the DeepFCM-ELM model is incorporated for the multimodal classification, improving diagnosis capabilities for both CAD and NSCLC. Heatmaps are developed, where the pathological regions are highlighted to interpret the decision-making process of CNNs, as has been demonstrated in previous study [4]. Natural Language Generation (NLG) is achieved by incorporating GPT to transform DeepFCM results into human-readable language, to enhance the transparency of the model's outcomes, as illustrated in [4].

The remainder of the paper is organized as follows: Section 2 details the methods and methodology, Section 3 presents the results, Section 4 discusses the findings, and Section 5 concludes with the study's key outcomes.

## 2 Materials & Methodology

### 2.1 CAD Patient Data

A total of 2036 patients underwent gated—SPECT MPI using 99mTc–tetrofosmin on hybrid SPECT/CT systems between February 2018 and February 2022, at the Nuclear Medicine Department at the University Hospital of Patras. Attenuation correction was applied to all the gathered images. After ICA within 60 days and applying exclusion criteria, 594 patients were selected, with 43.82% CAD–positive. The ethical committee of the University General Hospital of Patras approved the data collection process protocol number 108/10–3–2022). The raw image data were tomographically reconstructed on a dedicated workstation (Xeleris 3, GE Healthcare, Chicago, IL, USA) using the Ordered Subset Expectation–Maximization (OSEM) algorithm with two iterations and ten subsets. The software (Xeleris 3.0513) automatically generated polar maps, which are 2D circular representations summarizing the results of the 3D tomographic slices. These polar maps were saved in Digital Imaging and Communications in Medicine (DICOM) format for further processing. The twenty-two clinical characteristics considered are 1. Sex, 2. Age, 3. BMI, 4. known CAD, 5. previous AMI, 6. previous PCI, 7. previous CABG, 8. previous STROKE, 9. Diabetes, 10. Smoking, 11. Hypertension, 12. Dyslipidemia, 13. Angiopathy, 14. Chronic Kidney Disease, 15. Family History of CAD, 16. Asymptomatic, 17. Atypical Symptoms, 18. ANGINA LIKE, 19. Dyspnea on Exertion, 20. Incident of Precordial Pain, and 21. ECG, along with the 22. Expert Diagnosis (see [7]).

### 2.2 NSCLC Patient Data

PET/CT imaging was applied at the University Hospital of Patras with the Discovery iQ3 sl16 hybrid PET/CT scanner, in order to capture 3D whole-body volumes in a supine position of patients

with a 15 cm field of view. Two nuclear experts with significant experience (N.P., 10 years of experience, D.J.A., 30 years of experience) classified SPN malignancy through patient follow-up. The study was performed with obtaining patients' informed consent. From 2020 to 2023 period over 800 scans were gathered and reviewed, with 456 patients selected based on criteria excluding SPNs over 30 mm, where222 benign and 234 malignant cases were included. Experts annotated CT scan slices, providing the finding's type, location, margins, diameter, and SUVmax and SPN diameter along with demographic information about each patient (gender, age, BMI). The SUVmax and diameter parameters were extracted from the PET scan. Each SPN finding is represented by a single 2D slice in which the full demonstration of the SPN nodule is visible.

## 2.3 Deep Fuzzy Cognitive Map Methodology

The DeepFCM method has been introduced in previous studies and has been applied for the diagnosis of CAD using Polar Maps and for NSLC diagnosis using PET images (see [3]) and attained exceptional results, while offering interpretability of results. The DeepFCM approach combines the transparency of Fuzzy Cognitive Maps (FCMs) with the feature extraction capabilities of CNNs to form a holistic prediction, based on both clinical and imaging data. The clinical data obtained from each study are treated as input concepts from the FCM classifier to model the influence between the clinical factors, and the diagnosis [6]. RGB-CNN refers to a CNN, which has been implemented from scratch and tailored for each study and has been developed in previous studies for image classification tasks. In this research, RGB-CNN is trained to the Polar Maps images for CAD diagnosis and CT images for NSCLC diagnosis to predict the outcome of each image instance. Combined with the associated clinical data, these CNN predictions form the multimodal dataset for the DeepFCM framework, leveraging the strengths of both deep learning and FCM in handling complex medical data for more accurate predictions and insights. This study integrated ELM for the DeepFCM learning process to calculate concept interconnections.

*2.3.1 Proposed ELM Algorithm for DeepFCM Training Process.* Extreme Learning Machine is a training algorithm by Huang et al. [5] and was initially designed for training single hidden layer feedforward neural networks (SLFNs). Its different approach from traditional neural networks that demand fine-tuning of parameters, is highly advantageous. In ELM, hidden weights are randomly generated, preventing the necessity for additional adjustments. ELM's training process typically involves random filter mapping, wherein weights and biases undergo random generation. ELM also includes linear parameter solving, where output weights are determined by minimizing errors. A pivotal challenge of ELM lies in its capacity to attain minimal training error and output weights with the minimum norm.

Based on previous studies [5], [10], ELM has been applied in medical imaging tasks and has demonstrated time efficiency throughout its computational process.

Regarding the adaptation of ELM in the FCM learning process, ELM calculates the interconnections between concepts, ultimately improving the model's prediction capability, by initializing a set of random weights for the input layer or in our case based on expert knowledge, then passing the input data through the hidden layer, and calculating the hidden layer output using a dot product. The output weights are computed with the Moore-Penrose pseudoinverse equation. In the FCM learning process, the weights between concepts are iteratively updated using ELM predictions. The goal is to minimize the Mean Squared Error (MSE) between the actual and predicted outputs by adjusting the weights with the application of regularization techniques. The learning rate and regularization parameters are used to guide the weight adjustments, ensuring that the model converges toward an optimal solution. Through these steps, ELM enhances the FCM's ability to model complex relationships and improve diagnostic accuracy. The pseudocode of ELM integrated into DeepFCM learning is presented.

**Algorithm 1** ELM integration into DeepFCM learning

Step 1: Initialization of the DeepFCM structure
Define the DeepFCM nodes and initialize weighted relationships among concepts
Step 2: ELM structure
Select ELM parameters: number of hidden neurons, activation function, and learning rate
Initialize ELM weights and biases randomly/based on expert knowledge
Step 3: Training Loop
Update the activation levels of DeepFCM nodes with Kosko's inference equation
Integrate ELM training
Train DeepFCM through the ELM network using DeepFCM concepts as ELM input nodes
Calculate ELM hidden layer output $H = X \cdot W_n^T$
  Update ELM weights based on training error (MSE)
  Calculate output weights based on the Moore-Penrose pseudoinverse $W_{out} = H^+ \cdot Y$
  Optimize interconnections based on $W_{out} = W_{fcm} + \eta \cdot [(Y_{real} - Y_{elm}) \cdot Y_{elm} \cdot (1 - Y_{elm})]^T$
end

*2.3.2 Inference Process.* The weight matrix, which represents the influence and relationships among various clinical and imaging factors in the context of CAD and NSCLC diagnosis is calculated by ELM. During training, the DeepFCM-ELM model adjusts these weights to minimize error and optimize performance, effectively learning from expert knowledge. Once the learning process is terminated, and the final interconnections among concepts have been calculated the weight matrix is applied to the testing dataset, enabling the model to evaluate new instances based on the learned interconnections.

Heatmaps are generated using the Gradient-weighted Class Activation Mapping (Grad-CAM) technique, as implemented by Selvaraju [11]. Since the fully connected layers of a CNN lose spatial information, Grad-CAM leverages the feature maps from the final convolutional layer to highlight the most influential pixel regions. Natural Language Generation (NLG) is employed by creating a prompt, which is then processed by the GPT-API, an Application Programming Interface provided by OpenAI that leverages the Generative Pre-trained Transformer 4 (GPT-4) to transform the

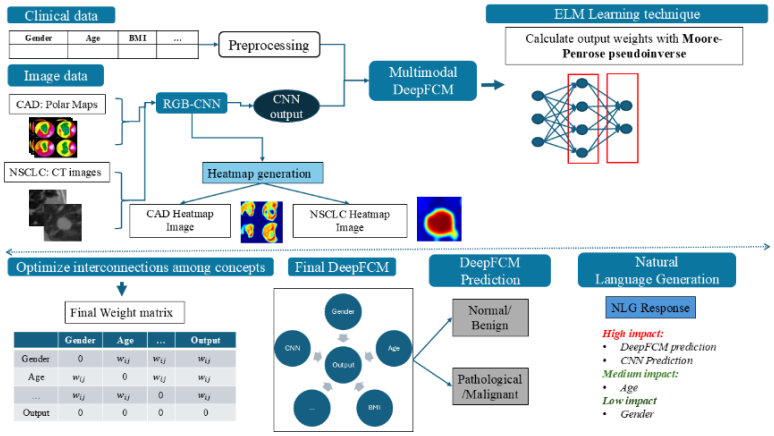


**Figure 1: Demonstration of the DeepFCM methodological pipeline applicable to CAD and NSCLC diagnosis**

**Table 1: Results obtained with RGB-CNN to Polar Maps image dataset and <strike>with</strike> DeepFCM as a multimodal approach for CAD diagnosis**

| Model | Accuracy | Loss | Sensitivity | Specificity | Precision |
|---|---|---|---|---|---|
| RGB-CNN | 75.58%±5.25% | 0.45±0.04 | 81.72%±5.59% | 65.48%±9.52% | 72%±7.85% |
| DeepFCM-GA | 78.29%±6.05% | 0.22±0.06 | 77.86%±10.47% | 75.67%±11.41% | 78.82%±6.89% |
| DeepFCM-ELM | 80.4%±4.97% | 0.19±0.05 | 75.47%±11.07% | 83.75%±14.33% | 73.98%±8.49% |

**Table 2: Results attained with RGB-CNN to CT image dataset and <strike>with</strike> DeepFCM as a multimodal approach for NSCLC diagnosis**

| Model | Accuracy | Loss | Sensitivity | Specificity | Precision |
|---|---|---|---|---|---|
| RGB-CNN | 84.69%±5.97% | 0.45±0.14 | 85.24%±11.8% | 79.11%±11.54% | 86.39%±9.13% |
| DeepFCM-GA | 85.71%±4.53% | 0.14±0.04 | 79.52%±13.89% | 90.17%±10.22% | 86.8%±4.09% |
| DeepFCM-ELM | 90.57%±3.07% | 0.08±0.03 | 81.9%±10.56% | 96%±5.47% | 89.21%±5.06% |

DeepFCM results into human-readable explanations for nuclear physicians. This prompt incorporates the clinical values of the respective patient, the heatmap visualization, which refers to the interpretation of CNN predictions [4], [9] the interconnections among concepts generated from DeepFCM, and the CNN and DeepFCM predictions for the particular patient. Figure 1 demonstrates the proposed DeepFCM methodological pipeline.

## 3 Results

### 3.1 Classification results

Robust evaluation metrics have been employed, including accuracy, loss, sensitivity, specificity, and precision, to demonstrate a clear comparison among the classification abilities of the developed models. 10-fold cross-validation is used, where the dataset is divided into 10 subsets, where the model is trained on 9 subsets and validated to the remaining one until all subsets have been utilized as the validation set.

Table 1 shows the performance of RGB-CNN, which has been trained to the CAD Polar Maps images only, along with DeepFCM-GA, and DeepFCM-ELM, which are multimodal approaches incorporating Genetic Algorithm (GA) and ELM as learning techniques. In Table 2, the same experiments have been conducted, using the CT images for NSCLC diagnosis.

Based on the attained results from Table 1 and Table 2 for the CAD diagnosis using Polar Maps, as well as for NSCLC diagnosis using CT images, it is demonstrated that the multimodal approaches, which combine clinical data and image predictions allow the model to capture a broader spectrum of information, ultimately leading to more robust and reliable predictions for both CAD and NSCLC.

More specifically, DeepFCM-ELM demonstrates superior performance compared to the multimodal approach DeepFCM-GA, for both case studies.

### 3.2 Figures

*3.2.1 Classification using DeepFCM-ELM..* To test the performance of DeepFCM-ELM, a 66-year-old male with a BMI of 23.8 patient was selected. His medical history includes known CAD, previous

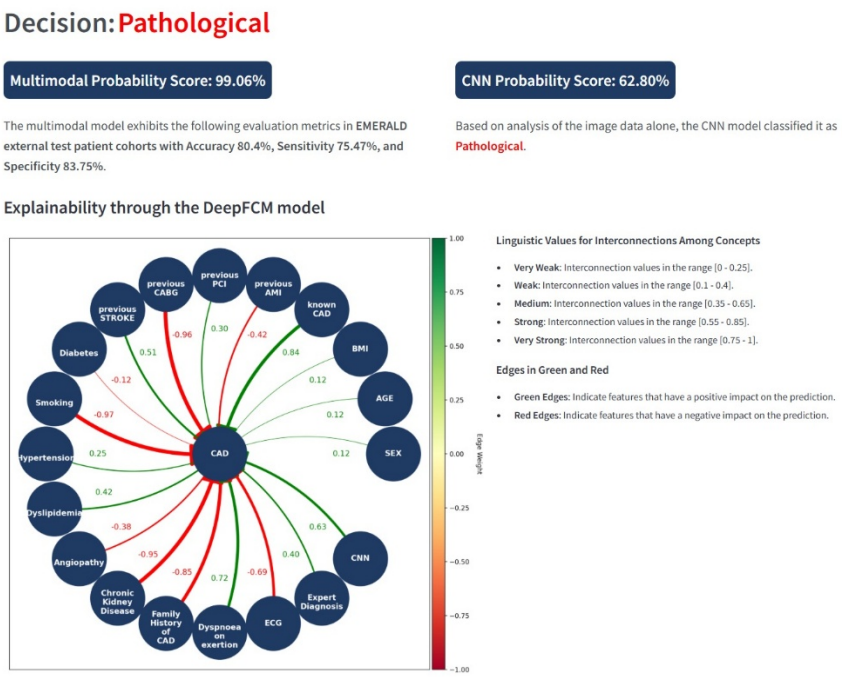


**Figure 2: Generated Interconnections of DeepFCM-ELM to Polar Maps Images for CAD Diagnosis**

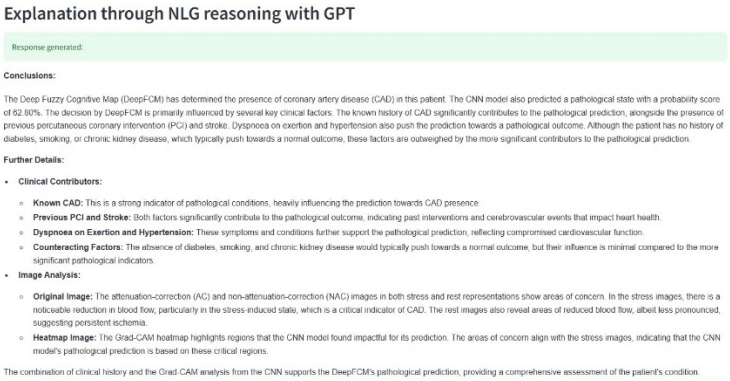


**Figure 3: NLG applied to CAD Diagnosis as XAI technique through MDSS**

Percutaneous Coronary Intervention (PCI), previous stroke, hypertension, dyslipidemia, and, he has dyspnea on exertion, which experts have predicted as pathological. Figure 2 illustrates that through the developed MDSS, DeepFCM-ELM has diagnosed him as pathological, based on the provided Polar Map image with a probability score of 62.8% and based on the multimodal approach with a probability score of 99.06%. Furthermore, the interconnections are demonstrated for the CAD diagnosis, combining clinical data with Polar Maps as imaging inputs, where dyslipidemia and CNN prediction have the highest influences for CAD diagnosis.

*3.2.2 Natural Language Generation Inference.* NLG reasoning is applied to interpret DeepFCM results, as demonstrated in Figure 3. A prompt is constructed that incorporates DeepFCM interconnections, CNN and DeepFCM predictions, and the values of the clinical parameters. A clear analysis is presented of the contribution of the clinical parameters and the provided image and heatmap visualization for the CAD diagnosis.

## 3.3 NSCLC diagnosis

*3.3.1 Classification using DeepFCM-ELM..* Regarding NSCLC diagnosis with the application of DeepFCM-ELM, we considered a patient case with the following characteristics: a 62-year-old female with a BMI of 33.3, a blood glucose level of 101.1, and an SUVmax of 2.0. The SPN measures 1.07 cm in diameter and is located in the right lower lobe. Figure 4 presents the diagnosis, where RGB-CNN as a stand-alone model predicted this instance as malignant, with a

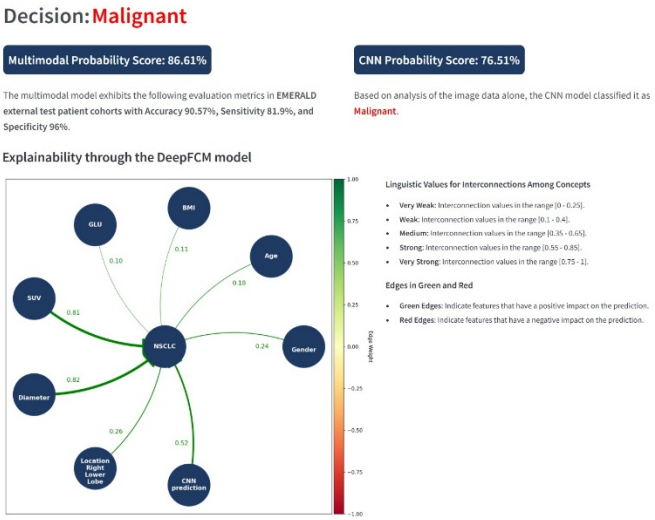


**Figure 4: Generated Interconnections of DeepFCM-ELM to CT Images for NSCLC Diagnosis**

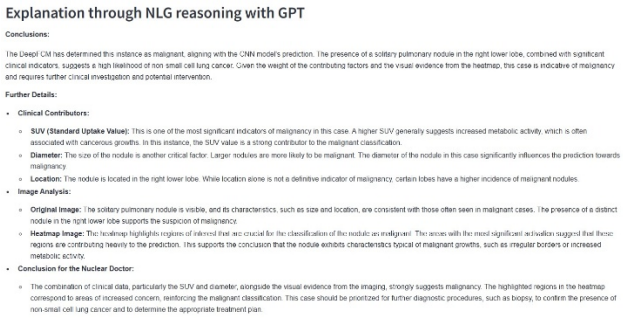


**Figure 5: NLG applied to NSCLC Diagnosis through MDSS**

probability score of 76.51%, and DeepFCM-ELM as a multimodal approach predicted this instance as malignant with a probability score of 86.61% based on the clinical values and the CT image. Also, the interconnections generated by the DeepFCM-ELM model are demonstrated, where SUVmax, diameter, and CNN prediction have the highest influence on NSCLC diagnosis.

*3.3.2 Natural Language Generation Inference.* NLG was applied to the NSCLC diagnostic process to interpret the decision-making process of DeepFCM-ELM, as illustrated in Figure 5. DeepFCM has classified the patient's SPN as malignant, consistent with the CNN model's prediction, indicating a high likelihood of malignancy.

## 4 Discussion

In this study, we applied DeepFCM to the diagnosis of CAD and NSCLC through the developed MDSS, using two distinct learning techniques: Genetic Algorithm and Extreme Learning Machine. Both GA and ELM were integrated into the FCM learning process to calculate the interconnections between input-output concepts derived from clinical data and CNN predictions. They proved their capacity to adapt to the training process of DeepFCM, offering a robust framework for integrating clinical data and image-based predictions. ELM offered a more structured approach by simplifying the learning process, leading to faster convergence times, and demonstrated slightly superior performance in CAD and NSCLC diagnosis. The generated interconnections among concepts revealed the influence of each attribute on the final diagnosis, leveraging the ability of FCMs. With the visualization of heatmaps, DeepFCM demonstrates the most impactful pixel regions of the images, revealing the calculations behind CNN's decision-making process. Moreover, NLG was employed to further enhance the interpretability of the DeepFCM results by transforming the complex outputs of DeepFCM into human-accepted explanations. These explanations bridge the gap between the developed AI techniques and the clinical applications.

However, this study includes certain limitations. Although the datasets for CAD and NSCLC diagnosis included a sufficient number of instances, they were sourced from a single hospital. Including data from different regions could enhance the generality of the proposed algorithms. Furthermore, even though DeepFCM-ELM demonstrated superior performance, the strengths of the rest of the models derived from literature studies could be examined. DeepFCM-GA achieved higher precision in CAD diagnosis, while RGB-CNN exhibited higher sensitivity. These strengths suggest opportunities to further experiment with DeepFCM-ELM's methodology and architecture to balance these metrics.

## 5 Conclusions

DeepFCM proves to be a highly effective approach since it delivered strong performance metrics for both case studies, which highlights its potential for broader clinical application. The application of two learning techniques, Genetic Algorithms, and Extreme Learning Machine demonstrates the capability of DeepFCM to be applied to different learning methods. Additionally, the explainability included in the DeepFCM classification process significantly enhances its trustworthiness, as it allows medical professionals to

validate the model's predictions, by demonstrating its clear decision-making process, with the interconnections among concepts, the heatmap generation, and the transformation of results in human-understandable language. In future work, the research team aims to broaden the provided approach to a wider variety of medical classification problems and enhance the methodology of natural language generation.

## Acknowledgments

The research project was supported by the Hellenic Foundation for Research and Innovation (H.F.R.I.) under the "2nd Call for H.F.R.I. Research Projects to support Faculty Members & Researchers" (Project Number: 3656). The source code can be found in [16].

## References

[1] Mehdi Amini, Mohamad Pursamimi, Ghasem Hajianfar, Yazdan Salimi, Abdollah Saberi, Ghazal Mehri-Kakavand, Mostafa Nazari, Mahdi Ghorbani, Ahmad Shalbaf, Isaac Shiri, and Habib Zaidi. 2023. Machine learning-based diagnosis and risk classification of coronary artery disease using myocardial perfusion imaging SPECT: A radiomics study. *Sci Rep* 13, 1 (September 2023), 14920. https://doi.org/10.1038/s41598-023-42142-w

[2] Asma Baccouche, Begonya Garcia-Zapirain, Cristian Castillo Olea, and Adel Elmaghraby. 2020. Ensemble Deep Learning Models for Heart Disease Classification: A Case Study from Mexico. *Information* 11, 4 (April 2020), 207. https://doi.org/10.3390/info11040207

[3] Anna Feleki, Ioannis D. Apostolopoulos, Elpiniki Papageorgiou, Serafeim Moustakidis, Nikolaos D. Papathanasiou, Dimitris J. Apostolopoulos, Konstantinos Kokkinos, and Nikolaos Papandrianos. 2023. Deep Fuzzy Cognitive Map methodology for Non-Small Cell Lung Cancer diagnosis based on Positron Emission Tomography imaging. In *2023 14th International Conference on Information, Intelligence, Systems & Applications (IISA)*, July 2023. 1–6. https://doi.org/10.1109/IISA59645.2023.10345912

[4] Anna Feleki, Ioannis Apostolopoulos, Serafeim Moustakidis, Elpiniki Papageorgiou, Nikolaos Papathanasiou, Dimitrios Apostolopoulos, and Nikolaos Papandrianos. 2023. Explainable Deep Fuzzy Cognitive Map Diagnosis of Coronary Artery Disease: Integrating Myocardial Perfusion Imaging, Clinical Data, and Natural Language Insights. *Applied Sciences* 13, (November 2023), 11953. https://doi.org/10.3390/app132111953

[5] Guang-Bin Huang, Qin-Yu Zhu, and Chee-Kheong Siew. 2006. Extreme learning machine: Theory and applications. *Neurocomputing* 70, 1 (December 2006), 489–501. https://doi.org/10.1016/j.neucom.2005.12.126

[6] L.S. Jayashree, R. Lakshmi Devi, Nikolaos Papandrianos, and Elpiniki I. Papageorgiou. 2018. Application of Fuzzy Cognitive Map for geospatial dengue outbreak risk prediction of tropical regions of Southern India. *Int. Dec. Tech.* 12, 2 (January 2018), 231–250. https://doi.org/10.3233/IDT-180330

[7] Nikolaos I. Papandrianos, Ioannis D. Apostolopoulos, Anna Feleki, Dimitris J. Apostolopoulos, and Elpiniki I. Papageorgiou. 2022. Deep learning exploration for SPECT MPI polar map images classification in coronary artery disease. *Ann Nucl Med* 36, 9 (September 2022), 823–833. https://doi.org/10.1007/s12149-022-01762-4

[8] Nikolaos I. Papandrianos, Ioannis D. Apostolopoulos, Anna Feleki, Serafeim Moustakidis, Konstantinos Kokkinos, and Elpiniki I. Papageorgiou. 2023. AI-based classification algorithms in SPECT myocardial perfusion imaging for cardiovascular diagnosis: a review. *Nucl Med Commun* 44, 1 (January 2023), 1–11. https://doi.org/10.1097/MNM.0000000000001634

[9] Nikolaos I. Papandrianos, Anna Feleki, Serafeim Moustakidis, Elpiniki I. Papageorgiou, Ioannis D. Apostolopoulos, and Dimitris J. Apostolopoulos. 2022. An Explainable Classification Method of SPECT Myocardial Perfusion Images in Nuclear Cardiology Using Deep Learning and Grad-CAM. *Applied Sciences* 12, 15 (January 2022), 7592. https://doi.org/10.3390/app12157592

[10] Geraldo Ramalho, Pedro Pedrosa Filho, Fatima Medeiros, and Paulo Cortez. 2014. Lung Disease Detection Using Feature Extraction and Extreme Learning Machine. *RBEB* 30, (December 2014), 207. https://doi.org/10.1590/rbeb.2014.019

[11] Ramprasaath R. Selvaraju, Michael Cogswell, Abhishek Das, Ramakrishna Vedantam, Devi Parikh, and Dhruv Batra. 2020. Grad-CAM: Visual Explanations from Deep Networks via Gradient-based Localization. *Int J Comput Vis* 128, 2 (February 2020), 336–359. https://doi.org/10.1007/s11263-019-01228-7

[12] Anil Kumar Swain, Aleena Swetapadma, Jitendra Kumar Rout, and Bunil Kumar Balabantaray. 2024. Classification of non-small cell lung cancer types using sparse deep neural network features. *Biomedical Signal Processing and Control* 87, (January 2024), 105485. https://doi.org/10.1016/j.bspc.2023.105485

[13] Writing Group Members, Dariush Mozaffarian, Emelia J. Benjamin, Alan S. Go, Donna K. Arnett, Michael J. Blaha, Mary Cushman, Sandeep R. Das, Sarah de Ferranti, Jean-Pierre Després, Heather J. Fullerton, Virginia J. Howard, Mark D. Huffman, Carmen R. Isasi, Monik C. Jiménez, Suzanne E. Judd, Brett M. Kissela, Judith H. Lichtman, Lynda D. Lisabeth, Simin Liu, Rachel H. Mackey, David J. Magid, Darren K. McGuire, Emile R. Mohler, Claudia S. Moy, Paul Muntner, Michael E. Mussolino, Khurram Nasir, Robert W. Neumar, Graham Nichol, Latha Palaniappan, Dilip K. Pandey, Mathew J. Reeves, Carlos J. Rodriguez, Wayne Rosamond, Paul D. Sorlie, Joel Stein, Amytis Towfighi, Tanya N. Turan, Salim S. Virani, Daniel Woo, Robert W. Yeh, Melanie B. Turner, American Heart Association Statistics Committee, and Stroke Statistics Subcommittee. 2016. Executive Summary: Heart Disease and Stroke Statistics–2016 Update: A Report From the American Heart Association. *Circulation* 133, 4 (January 2016), 447–454. https://doi.org/10.1161/CIR.0000000000000366

[14] Majd Zreik, Nikolas Lessmann, Robbert W. van Hamersvelt, Jelmer M. Wolterink, Michiel Voskuil, Max A. Viergever, Tim Leiner, and Ivana Išgum. 2018. Deep learning analysis of the myocardium in coronary CT angiography for identification of patients with functionally significant coronary artery stenosis. *Medical Image Analysis* 44, (February 2018), 72–85. https://doi.org/10.1016/j.media.2017.11.008

[15] HOME. *EMERALD*. Retrieved October 27, 2024 from https://emerald.uth.gr/

[16] elpinikipapageorgiou/EMERALD-3656ELIDEK-. *GitHub*. Retrieved February 16, 2025 from https://github.com/elpinikipapageorgiou/EMERALD-3656ELIDEK-